Inorg. Chem. **2005**, *44*, 4796–4805

Aromatic Interactions in Unusual Backbone Nitrogen-Coordinated Zinc Peptide Complexes: A Crystallographic and Spectroscopic Study

Slobodan Novokmet,[‡] Frank W. Heinemann,[‡] Achim Zahl,[‡] and Ralf Alsfasser*[,†]

Institute of Inorganic Chemistry, University of Freiburg, Albertstr. 21, D-79104 Freiburg, Germany, and Institute of Inorganic Chemistry, University of Erlangen-Nürnberg, Egerlandstr. 1, D-91058 Erlangen, Germany

Received January 3, 2005

A series of zinc complexes with dipeptide ligands of the type Dpg-Xaa was synthesized, where Dpg is dipicolylglycine and Xaa is phenylalanine (Phe), tyrosine (Tyr), tryptophan (Trp), 2-naphthylalanine (Nal), or glycine (Gly). It was shown that aromatic interactions promote the unusual coordination of an anionic peptide backbone nitrogen atom to zinc. This binding mode was, for the first time, characterized by X-ray structure analyses of the electrically neutral complexes [(Dpg-Phe)$^{-H}$Zn], [(Dpg-Tyr)$^{-H}$Zn], [(Dpg-Trp)$^{-H}$Zn], and [(Dpg-Nal)$^{-H}$Zn]. The pK_a values for amide nitrogen deprotonation were determined by ^{1}H NMR titrations {[(Dpg-Phe)Zn], 7.17; [(Dpg-Tyr)Zn], 6.85; [(Dpg-Trp)Zn], 6.85; [(Dpg-Nal)Zn], 6.64; [(Dpg-Gly)Zn], 8.54}. It was calculated that aromatic interactions contribute ca. −8 to −11 kJ/mol of stabilizing free enthalpy changes in the derivatives with aromatic amino acid side chains. These are the first quantitative data obtained for crystallographically characterized metal complexes. A comparison with the literature shows that it is difficult to distinguish between π–cation attraction and π–π stacking. However, it is evident that modification of small peptides with synthetic pyridine ligands enhances their ability to stabilize secondary structures by noncovalent interactions. This is an important consideration for the design of biomimetic metallopeptides.

Introduction

Weak noncovalent aromatic interactions are ubiquitous in biological systems as well as in synthetic supramolecular compounds.[1] In their classic papers, Burley and Petsko have shown that aromatic amino acid side chains help stabilizing protein structures by a calculated free enthalpy change of ca. −4.2 to −8.4 kJ/mol.[2] Much higher stacking energies of more than −40 kJ/mol have been measured between porphyrin rings.[3] The large variation between different π systems and the difficulty in assessing the importance of electrostatic contributions and hydrophobic effects show that a classification based on experimental data is desirable.[4] However, a single aromatic interaction is difficult to study, particularly when amino acids are concerned. The energy is usually small and in most cases obscured by other effects. One possible method to obtain quantitative data is to compare chemically related species that allow the isolation of a single contribution in a thermodynamic cycle.[5]

This applies not only to organic compounds but also to metal complexes with aromatic substituents.[6] Such compounds are interesting, for example, because of their relevance for the structures and functions of metalloproteins[7] or their potential for the chiral discrimination between L and D amino acids.[8] However, most probably because of their kinetic lability, only a few papers have dealt with a quantitative determination of aromatic interactions in metal amino acid complexes. Yamauchi and co-workers have used

* To whom correspondence should be addressed. E-mail: ralf.alsfasser@ac.uni-freiburg.de.
† University of Freiburg.
‡ University of Erlangen-Nürnberg.

(1) (a) Waters, M. L. *Curr. Opin. Chem. Biol.* **2002**, *6*, 736. (b) Hunter, C. A.; Lawson, K. R.; Perkins, J.; Urch, C. J. *J. Chem. Soc., Perkin Trans. 2* **2001**, 651. (c) Ma, J. C.; Dougherty, D. A. *Chem. Rev.* **1997**, *97*, 1303.
(2) (a) Burley, S. K.; Petsko, G. A. *Science* **1985**, *229*, 23. (b) Burley, S. K.; Petsko, G. A. *J. Am. Chem. Soc.* **1986**, *108*, 7995.
(3) Hunter, C. A.; Meah, M. N.; Sanders, J. K. M. *J. Am. Chem. Soc.* **1990**, *112*, 5773.
(4) (a) Newcomb, L. F.; Gellmann, S. H. *J. Am. Chem. Soc.* **1994**, *116*, 4993. (b) Pang, Y.-P.; Miller, J. L.; Kollmann, P. A. *J. Am. Chem. Soc.* **1999**, *121*, 1717.
(5) (a) Adams, H.; Carver, F. J.; Hunter, C. A.; Morales, J. C.; Seward, E. M. *Angew. Chem., Int. Ed. Engl.* **1996**, *35*, 1542. (b) Bisson, A. P.; Hunter, C. A. *J. Chem. Soc., Chem. Commun.* **1996**, 1723. (c) Adams, H.; Harris, K. D. M.; Hembury, G. A.; Hunter, C. A.; Livingstone, D.; McCabe, J. F. *J. Chem. Soc., Chem. Commun.* **1996**, 2531.
(6) (a) Janiak, C. *J. Chem. Soc., Dalton Trans.* **2000**, 3385. (b) Yamauchi, O.; Odani, A.; Takani, M. *J. Chem. Soc., Dalton Trans.* **2002**, 3411.
(7) Zaric, S. D. *Eur. J. Inorg. Chem.* **2003**, 2197.

10.1021/ic0500053 CCC: $30.25 © 2005 American Chemical Society
Published on Web 05/25/2005

Scheme 1. Synthesis of the N-Coordinated Zinc Peptide Complexes **6**−**10**

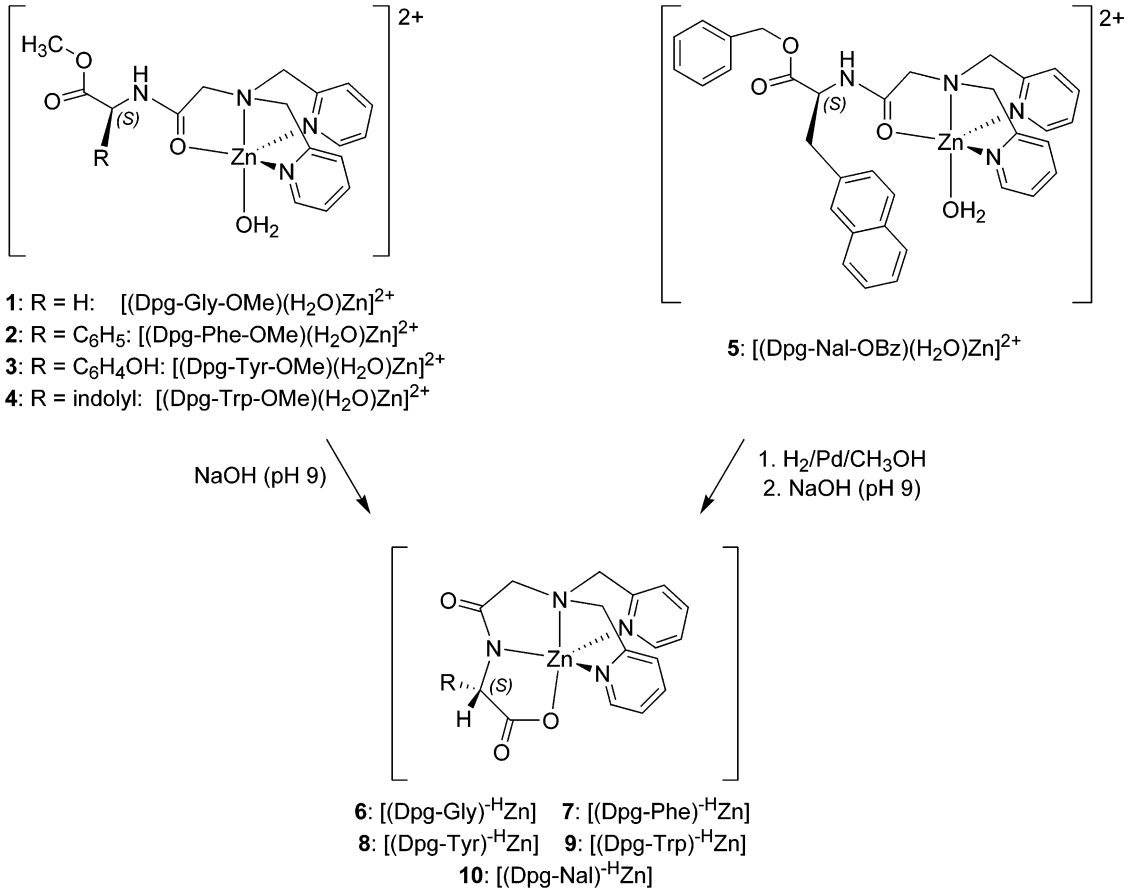

the formation constants of ternary amino acid complexes to calculate free enthalpy changes of −3.6 to −7.9 kJ/mol in copper(II) species[9] and −2.1 to −9.7 kJ/mol in palladium(II)[10] species. The methodology followed earlier papers by Sigel et al., who reported $\Delta\Delta\log K$ values as measures for aromatic interactions in ternary copper(II) complexes and zinc(II) complexes but stated that calculated differences between stability constants are rather inaccurate.[11] Fabbrizzi et al. have used a fluorescent anthracene substituted zinc complex as a sensor for phenylalanine and tryptophan.[12] Titration experiments were performed to obtain anthracene−phenyl and anthracene−indolyl interaction energies of −8 and −7 kJ/mol, respectively. To the best of our knowledge, there is no report on quantitative data for structurally characterized coordination complexes.

Here, we present the first examples as a part of our work on zinc(II) complexes with bioinorganic hybrid ligands containing a dipicolylamine unit in a dipeptide framework.[13] Intramolecular aromatic interactions between a pyridine ligand and an aromatic amino acid side chain are shown to promote the deprotonation and coordination of a peptide nitrogen atom. This is unprecedented for zinc peptide complexes and was confirmed by X-ray crystallography. Acidification and protonation triggers carbonyl oxygen coordination, which is accompanied by a structural reorganization with a complete loss of π stacking in aqueous solutions. NMR−pH-titration experiments afforded pK_a values, which were used to calculate the free enthalpy changes brought about by aromatic interactions involving different amino acid side chains.

Results and Discussion

Synthesis of N-Coordinated Zinc Peptide Complexes. Scheme 1 shows the compounds investigated in this paper. The starting materials were zinc complexes of dipeptide ester ligands containing the chelating amino acid dipicolylglycine (Dpg). Their synthesis followed our earlier report on the glycine ethyl ester complex $[(Dpg\text{-}Gly\text{-}OEt)(H_2O)Zn]^{2+}$ (**1′**) and the phenylalanine methyl ester complex $[(Dpg\text{-}Phe\text{-}OMe)(H_2O)Zn]^{2+}$ (**2**).[13] To compare effects of different aromatic side chains, the tyrosine methyl ester (**3**), tryptophan methyl ester (**4**), and 2-naphthylalanine benzyl ester (**5**) derivatives were prepared. To apply the complexes in peptide coupling reactions, we removed the methyl ester functions in **1**−**4** under basic conditions at pH 9. Surprisingly, this

(8) Jitsukawa, K.; Katoh, A.; Funato, K.; Ohata, N.; Funahashi, Y.; Ozawa, T.; Masuda, H. *Inorg. Chem.* **2003**, *42*, 6163.
(9) Yamauchi, O.; Odani, A. *J. Am. Chem. Soc.* **1985**, *107*, 5938.
(10) Odani, S.; Deguchi, S.; Yamauchi, O. *Inorg. Chem.* **1986**, *25*, 62.
(11) (a) Fischer, B. E.; Sigel, H. *J. Am. Chem. Soc.* **1980**, *102*, 2998. (b) Malini-Balakrishnan, R.; Scheller, K. H.; Häring, U. K.; Tribolet, R.; Sigel, H. *Inorg. Chem.* **1985**, *24*, 2067.
(12) Fabbrizzi, L.; Licchelli, M.; Perotti, A.; Poggi, A.; Rabaioli, G.;. Sacchi, D.; Taglietti, A. *J. Chem. Soc., Perkin Trans. 2* **2001**, 2108.
(13) (a) Niklas, N.; Walter, O.; Alsfasser, R. *Eur. J. Inorg. Chem.* **2000**, 1723. (b) Niklas, N.; Zahl, A.; Alsfasser, R. *J. Chem Soc., Dalton Trans.* **2003**, 778. (c) Niklas, N.; Walter, O.; Hampel, F.; Alsfasser, R. *J. Chem. Soc., Dalton Trans.* **2002**, 3367.

Scheme 2. pH-Dependent Equilibrium between N-Coordinated and O-Coordinated Complexes

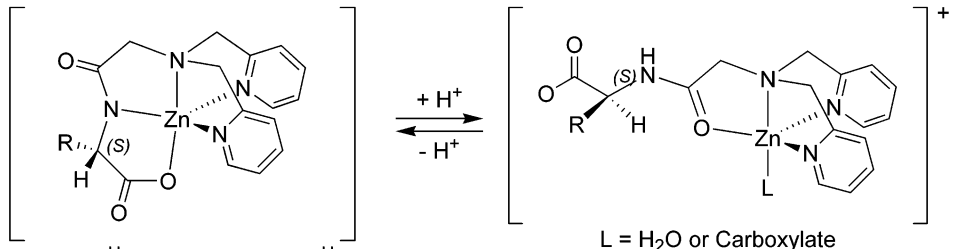

6: [(Dpg-Gly)$^{-H}$Zn] **7**: [(Dpg-Phe)$^{-H}$Zn]
8: [(Dpg-Tyr)$^{-H}$Zn] **9**: [(Dpg-Trp)$^{-H}$Zn]
10: [(Dpg-Nal)$^{-H}$Zn]

6a: [(Dpg-Gly)(L)Zn] **7a**: [(Dpg-Phe)(L)Zn]
8a: [(Dpg-Tyr)(L)Zn] **9a**: [(Dpg-Trp)(L)Zn]
10a: [(Dpg-Nal)(L)Zn]

resulted not only in the coordination of the free carboxylate function but also in the deprotonation and coordination of the amide nitrogen atom. The electrically neutral distorted trigonal-bipyramidal complexes **6**−**9** were formed (see Scheme 2). For [(Dpg-Phe)$^{-H}$Zn] (**7**), [(Dpg-Tyr)$^{-H}$Zn] (**8**), and [(Dpg-Trp)$^{-H}$ Zn] (**9**), single crystals were grown and the structures confirmed by X-ray diffraction. The benzyl ester function in **5** was removed by catalytic hydrogenation in methanol. The complex [(Dpg-Nal)$^{-H}$Zn] (**10**) formed after dissolving the product in aqueous NaOH at pH 9. It was also characterized by X-ray structure analysis.

Protonation of the amide function in **6**−**10** with hydrochloric acid triggers a rearrangement of the dipeptide ligand, which now binds via its carbonyl oxygen atom (**6a**−**10a**). This reaction is interesting because coordination of the free carboxylate function in **7a**−**10a** resulted in the precipitation of a new class of homochiral, right-handed helical coordination polymers.[14] We have studied their aggregation on graphite substrates by scanning tunneling microscopy in order to characterize the effects of amino acid side chains and the local surface environment on structure formation processes.[15] The glycine **6a** derivative does not polymerize but forms the cyclic tetramer $\{[(Dpg\text{-}Gly)Zn](CF_3SO_3)\}_4$.[16] The pH-dependent switching of the amide group coordination mode is fully reversible in all cases and can be conveniently monitored by ^{1}H NMR spectroscopy. Following a description of the crystal structures of **8**−**10**, we will discuss how this property was used for a quantitative evaluation of aromatic interaction energies.

It should be noted that the nitrogen coordinated complexes **6**−**10** are most conveniently synthesized by treating the solid polymers with aqueous NaOH at pH 9 (see Experimental Section). The latter are easy to purify from organic materials, which is important for the quality of the NMR studies described below. However, fast atom bombardment (FAB) mass spectrometry and IR spectroscopy showed that the so-obtained samples always contained variable amounts of Na(CF_3SO_3), which could not be removed. Because this did not influence the relevant properties of the compounds, all experiments including crystallization were performed with these samples. The tryptophan derivative **9**, which was the most difficult to purify, was also synthesized using an alternative route starting from $ZnCl_2$. The method is described in the Experimental Section. Although the samples yielded better elemental analysis data, they always contained 2 equivs of methanol that could not be removed by extended drying under a vacuum and affected the interpretation of NMR spectra in the aliphatic region.

Structures. Before we discuss the key feature, the anionic nitrogen coordination of the peptide backbone, it is useful to look at some general properties. Crystallographic details are summarized in Table 1, and a comparison of selected structural parameters is given in Table 2. ORTEP plots of complexes **8**−**10** are shown in Figure 1.

The coordination mode of the tridentate dipicolylamine moiety is typical for zinc complexes of this ligand fragment.[17] However, compounds **7**, **8**, and **10** do not crystallize as mononuclear complexes. Figure 2 shows that they form distinctly different coordination polymers. In the phenylalanine and tyrosine derivatives **7** and **8**, infinite chains are built by the bridging of the two carboxylate oxygen donors. The zinc(II) center is, therefore, six-coordinate, which causes larger N2−Zn−N3 angles of 128.9° in **7** and 144.8° in **8** compared with 114.0° in **9** and 103.7° in **10**. A slight elongation of all zinc-to-ligand distances is also observed. The naphthylalanine derivative **10** cocrystallizes with 1 equiv of sodium triflate. The amide oxygen atom O1 as well as both carboxylate oxygen donors O2 and O3 bind to Na^+. A triflato ligand completes the distorted tetrahedral coordination sphere, which contains four different oxygen donor ligands. Interestingly, only the (*R*)-isomer is observed. The result is a band-type structure with a sodium triflate central part connecting two rows of **10**. The bridging function of sodium ions in coordination polymers is not unknown,[18] although we are not aware of any other example with a chiral coordination sphere around Na^+.

Unprecedented in structurally characterized zinc peptide complexes is the coordination of a deprotonated dipeptide nitrogen atom to zinc(II). Only a few related examples for zinc complexes with anionic carboxamide nitrogen ligands have been reported. The closest is a bleomycine model by

(14) Niklas, N.; Hampel, F.; Alsfasser, R. *Chem. Commun.* **2003**, 1586.
(15) Novokmet, S.; Alam, S.; Dremov, V.; Heinemann, F. W.; Müller, P.; Alsfasser, R. *Angew. Chem., Int. Ed.* **2005**, *44*, 803.
(16) An X-ray structure analysis confirms this structural assignment, but the data are only of poor quality.
(17) (a) Allen, C. S.; Chuang, C.-L.; Cornebise, M.; Canary, J. W. *Inorg. Chim. Acta* **1995**, *239*, 29. (b) Adams, H.; Bailey, N. A.; Fenton, D. E.; He, Q.-Y.; *J. Chem. Soc., Dalton Trans.* **1997**, 1533. (c) Burth, R.; Stange, A.; Schäfer, M.; Vahrenkamp, H. *Eur. J. Inorg. Chem.* **1998**, 1759. (d) Trosch, A.; Vahrenkamp, H. *Eur. J. Inorg. Chem.* **1998**, 827. (e) Niklas, N.; Wolf, S.; Liehr, G.; Anson, C. E.; Powell, A. K.; Alsfasser, R. *Inorg. Chim. Acta* **2001**, *314*, 126.

Table 1. Crystallographic Data for {**7**·2.5CH_3OH}$_\infty$, **8**$_\infty$, **9**·2.75H_2O, and {**10**·$NaCF_3SO_3$}$_\infty$

compound	{**7**·2.5 CH_3OH}$_\infty$	**8**$_\infty$	**9**·2.75 H_2O	{**10**·$NaCF_3SO_3$}$_\infty$
formula	$C_{25.5}H_{32}N_4O_{5.5}Zn$	$C_{23}H_{22}N_4O_4Zn$	$C_{25}H_{28.5}N_5O_{5.75}Zn$	$C_{28}H_{24}F_3N_4NaO_6SZn$
fw	547.92	483.82	556.40	689.93
cryst size [mm^3]	0.26 × 0.18 × 0.08	0.16 × 0.15 × 0.06	0.30 × 0.18 × 0.12	0.26 × 0.10 × 0.09
temp [K]	100(2)	100(2)	100(2)	100(2)
cryst syst	monoclinic	monoclinic	triclinic	orthorhombic
space group	*C*2	$P2_1$	*P*1	$P2_12_12_1$
a [Å]	22.035(2)	9.5772(6)	9.8276(6)	7.602(1)
b [Å]	8.9883(6)	9.4446(5)	10.7925(7)	16.215 (1)
c [Å]	13.1047(8)	10.7966(6)	13.3530(6)	23.130(2)
α [deg]	90	90	103.483(5)	90
β [deg]	100.373(5)	95.039(4)	108.767(4)	90
γ [deg]	90	90	101.066(5)	90
vol [Å^3]	2553.1(3)	972.8(1)	1248.0(2)	2851.2(3)
Z	4	2	2	4
D_{calcd} [mg/m^3]	1.425	1.652	1.481	1.607
μ [mm^{-1}]	1.007	1.305	1.034	1.020
θ range [deg]	3.35−28.70	3.48−27.51	3.47−26.02	3.65−28.70
measured reflns	28 183	16 929	25 211	34 429
independent reflns	6266 (R_{int} = 0.0358)	4471 (R_{int} = 0.0500)	9420 (R_{int} = 0.0382)	7296 (R_{int} = 0.0552)
observed reflns[a]	5724	3975	7904	5836
params	335	290	653	397
GOF on F^2	1.087	1.057	1.012	0.897
R_1 [a]	0.0309	0.0296	0.0470	0.0375
wR_2 (all data)	0.0844	0.0614	0.1096	0.0756
abs. struct. params[38]	0.02(1)	0.02(1)	0.02(2)	0.02(1)
$\Delta\rho_{max./min.}$ [*e* Å^{-3}]	0.756/−0.654	0.299/−0.379	0.988/−0.501	0.531/−0.331

[a] [$I > 2\sigma(I)$].

Table 2. Selected Bond Distances (Å) and Angles (deg) in the Structures of {[(Dpg-Phe)$^{-H}$Zn]·2.5CH_3OH}$_\infty$ ({**7**·2.5CH_3OH}$_\infty$), [(Dpg-Tyr)$^{-H}$Zn]$_\infty$ (**8**$_\infty$), [(Dpg-Trp)$^{-H}$Zn]·2.75H_2O (**9**·2.75H_2O), and {[(Dpg-Nal)$^{-H}$Zn]·Na(CF_3SO_3)}$_\infty$ ({**10**·Na(CF_3SO_3)}$_\infty$)

	{**7**·2.5CH_3OH}$_\infty$	**8**$_\infty$	**9**·2.75H_2O	{**10**·$NaCF_3SO_3$}$_\infty$
N1−Zn	2.358(2)	2.331(2)	2.264(3)	2.274(2)
N2−Zn	2.113(2)	2.085(2)	2.054(4)	2.062(2)
N3−Zn	2.168(2)	2.159(2)	2.032(4)	2.051(2)
N4−Zn	2.064(2)	2.036(2)	1.942(4)	1.963(2)
O2−Zn	2.102(1)	2.137(2)	2.044(4)	2.030(2)
O3[a]−Zn	2.139(2)	2.127(2)		
N1−Zn−N2	75.7(1)	78.4(1)	79.4(2)	79.2(1)
N1−Zn−N3	72.2(1)	74.4(1)	81.0(2)	79.7(1)
N1−Zn−N4	74.4(1)	78.4(1)	80.4(2)	78.4(1)
N1−Zn−O2	150.2(1)	156.2(1)	162.2(2)	159.0(1)
N1−Zn−O3[a]	131.8(1)	118.5(1)		
N2−Zn−N3	128.9(1)	144.8(1)	114.0(1)	103.7(1)
N2−Zn−N4	107.2(1)	99.8(1)	115.1(2)	122.9(1)
N2−Zn−O2	102.9(1)	103.8(1)	103.1(1)	104.4(1)
N2−Zn−O3[a]	89.27(1)	89.8(1)		
N3−Zn−N4	101.2(1)	96.2(1)	122.5(2)	122.6(1)
N3−Zn−O2	124.4(1)	110.1(1)	113.1(2)	118.5(1)
N3−Zn−O3[a]	83.7(1)	84.0(1)		
N4−Zn−O2	77.8(1)	77.9(1)	82.7(2)	82.5(7)
N4−Zn−O3[a]	152.8(1)	162.2(1)		
O2−Zn−O3[a]	77.4(1)	85.3(1)		
	Coordination Sphere around the Sodium Ion in {**10**·Na(CF_3SO_3)}$_\infty$			
Na−O1[b]	2.287(2)	O1[b]−Na−O3[c]	120.5(1)	
Na−O2	2.329(2)	O1[b]−Na−O11[d]	93.9(1)	
Na−O3[c]	2.303(2)	O2−Na−O3[c]	141.2(1)	
Na−O11[d]	2.377(2)	O2−Na−O11[d]	114.6(1)	
O1[b]−Na−O2	82.6(1)	O3[c]−Na−O11[d]	95.9(1)	

[a] **7**: $-x + 1/2, y + 1/2, -z$. **8**: $-x + 1, y - 1/2, -z + 2$. [b] $x - 1, y, z$. [c] $x - 1/2, -y + 1/2, -z$. [d] $-x - 1/2, -y + 1, z - 1/2$.

Goto et al., which resembles an Xaa−His complex.[19] Kimura et al. have applied the macrocyclic effect in a pyridine substitute cyclam amide derivative to support the amide nitrogen coordination.[20] Interestingly, the Zn−N^{amide} distances in both compounds are ca. 2.10 Å. This is significantly longer than in our dipeptide complexes, which have zinc nitrogen contacts of 1.94−2.04 Å. A comparable value of 1.97 Å has been reported by the Kimura group for a complex containing a relatively acidic nitrophenylamide moiety tethered to a cyclen ligand.[21]

(18) Examples: (a) Fu, Z.-Y.; Dai, J.-C.; Zhang, J.-J.; Hu, S.-M.; Fu, R.-B.; Du, W.-X.; Wu, X.-T. *Inorg. Chem. Commun.* **2003**, *6*, 919. (b) Chen, X.-Y.; Shi, W.; Cheng, P.; Chen, J.-T.; Yan, S.-P.; Liao, D.-Z.; Jiang, Z.-H. *Z. Anorg. Allg. Chem.* **2003**, *629*, 2034. (d) Pan, L.; Finkel, B. S.; Huang, X.-Y.; Li, J. *Chem. Commun.* **2001**, 105. (e) Zhang, L.; Cheng, P.; Tang, L.-F.; Weng, L.-H.; Jiang, Z.-H.; Liao, D.-Z.; Yan, S.-P.; Wang, G.-L. *Chem. Commun.* **2000**, 717. (f) Blake, A. J.; Fallis, I. A.; Gould, R. O.; Parsons, S.; Ross, S. A.; Schröder, M. *J. Chem. Soc., Chem. Commun.* **1994**, 2467.

(19) Kurosaki, H.; Hayashi, K.; Ishikawa, Y.; Goto, M. *Chem. Lett.* **1995**, 691.

(20) Kimura, E.; Koike, T.; Shiota, T.; Iitaka, Y. *Inorg. Chem.* **1990**, *29*, 4621.

(21) Kimura, E.; Gotoh, T.; Aoki, S.; Shira, M. *Inorg. Chem.* **2002**, *41*, 3239.

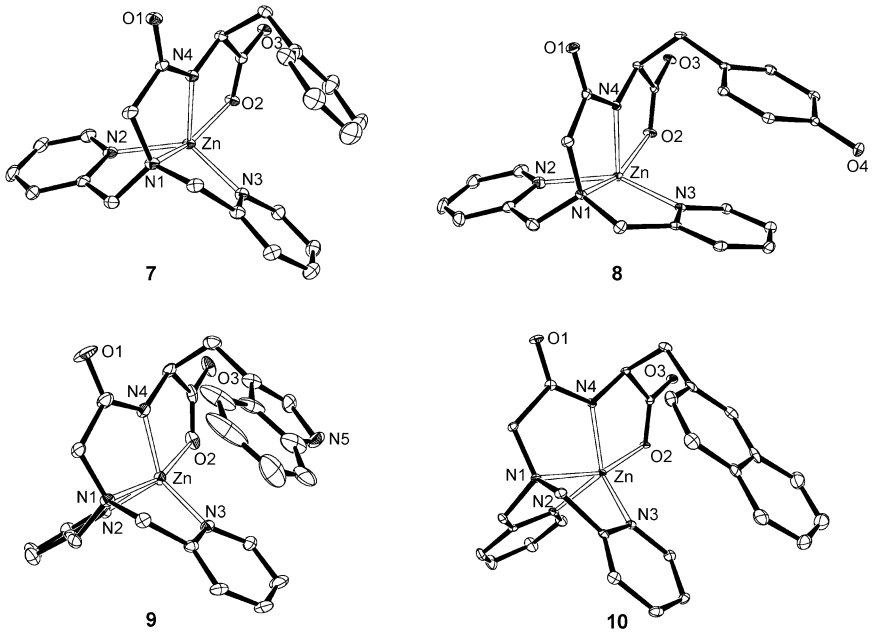

Figure 1. ORTEP representations (30% ellipsoids) of complexes **7**−**10** (hydrogen atoms omitted for clarity).

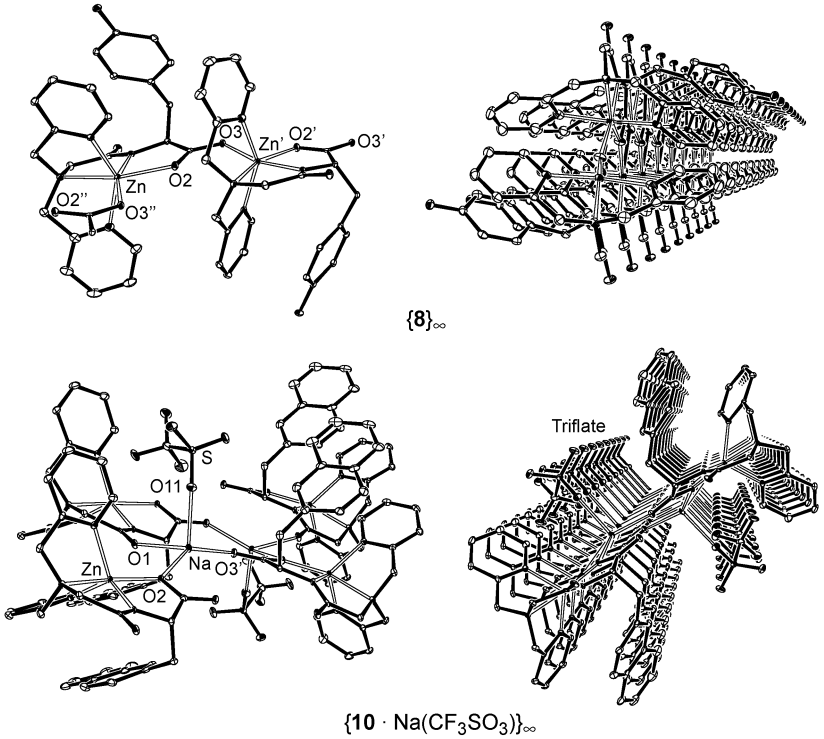

Figure 2. (top) Structure of {**8**}$_\infty$ illustrates how bridging of the carboxylate function between two zinc ions in **7** and **8** results in formation of coordination polymers. (bottom) A polymer containing *(R)*-configured distorted tetrahedral sodium atoms is formed when Na(CF_3SO_3) is coordinated by the amide and the two carboxylate oxygen atoms of **10**.

Peptide backbone coordination involving one or more deprotonated amide nitrogen donors has recently attracted much attention because of its role in the copper(II) binding sites of prion and Alzheimer proteins.[22] It also appears in the N-terminal nickel(II) and copper(II) binding ATCUN motif of proteins such as serum albumin.[23] That zinc(II) ions usually do not promote the deprotonation of peptide backbone nitrogen atoms is a long-accepted concept in metallopeptide chemistry.[24] The only exceptions are dipeptides of the type Xaa−His, were Xaa is a variable amino acid.[25] Interestingly, histidine may be replaced by bis(pyridine-2-yl)methylamine.[26] However, the heterocyclic amine donor must be at the C terminus because of the more favorable chelate ring.[24] No deprotonation is observed when the order of the peptide sequence changes. Thus, our compounds are unique not only because they are the first crystalline zinc(II) peptide complexes with an anionic backbone nitrogen

(22) Brown, D. R.; Kozlowski, H. *J. Chem Soc., Dalton Trans.* **2004**, 1907.
(23) Harford, C.; Sarkar, B. *Acc. Chem. Res.* **1997**, *30*, 123.
(24) Sigel, H.; Martin, R. B. *Chem. Rev.* **1982**, *82*, 385.

donor but also because the heterocyclic amine ligand is not at the C terminus but is instead at the N terminus. Their unexpected stability is, in part, certainly due to the coordinating carboxylate function and the concurrent formation of a five-membered chelate ring. However, a more interesting stabilizing factor is the observed stacking of the aromatic amino acid side chain with one of the pyridine ligands. The average distances between the aromatic planes are 3.7 Å in **7**, 3.4 Å in **8** and **9**, and 3.2 Å in **10**. To test the relevance of noncovalent interactions, we determined the pK_a values for the amide deprotonation in **6**−**10**. The glycine derivative **6** does not contain a side chain functional group but has a potentially coordinating terminal carboxylate function. It therefore provides a standard that enables us to single out the contribution of aromatic interactions to the stabilization of **7**−**10**.

^{1}H NMR Spectra in D_2O and the Determination of pK_a Values. A convenient way to perform pH-titration experiments with our complexes is by NMR spectroscopy in D_2O. In an earlier report on the formation of a helical coordination polymer from **7a**, we showed that the spectra at high and low pH* are distinctly different (pH* = pH-meter reading in D_2O solution without correction).[14] They are assignable to the amide N- and O-coordinated species, respectively. Figure 3 shows the spectra of the glycine derivatives **6**/**6a** (Figure 3a) and the phenylalanine derivatives **7**/**7b** (Figure 3b). Similar patterns were observed for the tyrosine, tryptophan, and naphthylalanine species **8**−**10** and **8a**−**10a**. Most informative are the high-field shifts of the C(O)−CH_2 group in all complexes, as well as those of the aromatic side chain and the pyridine $^{6'}$CH resonances in **7**−**10** at high pH. The former indicate that all complexes including the nonaromatic glycine derivative **6** have similar structures. The latter are characteristic for π stacking and confirm that the crystallographically determined conformation of the amino acid side chains is retained in solution. In contrast, no indication for stacking was observed in the spectra of the amide O-coordinated species **7a**−**10a** formed under acidic conditions. The aromatic proton resonances appear in the typical range of the free ligand signals without any significant shift. This is interesting because we had earlier observed a significant high-field shift of the methyl ester **2** in $CDCl_3$.[13] The differences cannot be explained on the basis of the available data, but it is safe to conclude that aromatic interactions are not relevant in D_2O solutions of **7a**−**10a** and that the pK_a values for amide deprotonation reflect the stabilization of the N-coordinated form by aromatic interactions.

Because the transition from amide O to N coordination occurs in the slow exchange regime, the integral of either an aromatic proton resonance or the C(O)−CH_2 group signal

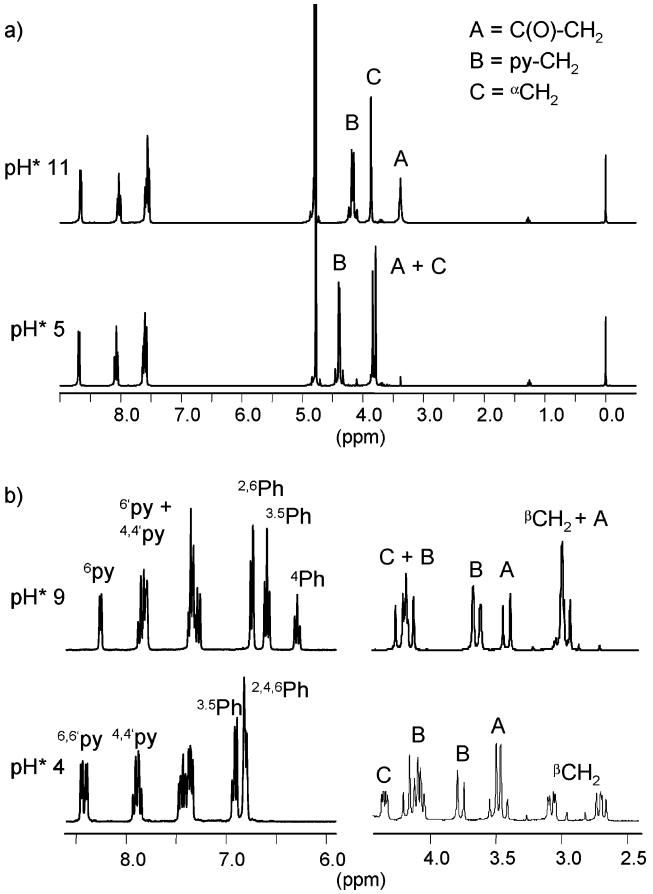

Figure 3. ^{1}H NMR spectra in D_2O/NaOD and D_2O/DCl of (a) the glycine derivatives **6** at pH* 11 and **6a** at pH* 5 and (b) the phenylalanine derivatives **7** at pH 9 and **7a** at pH* 4.

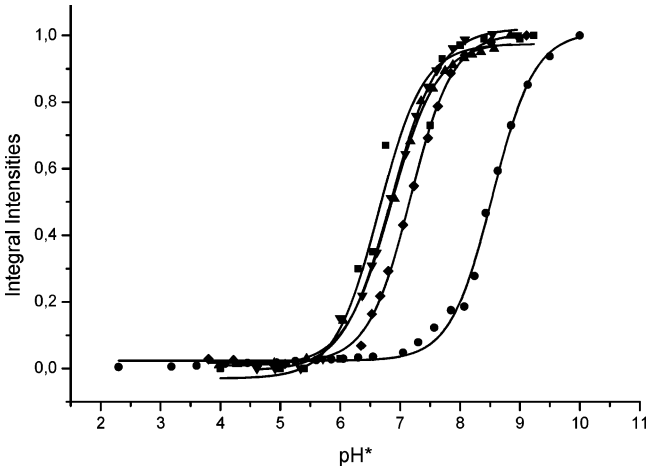

Figure 4. ^{1}H NMR titration curves for complexes **6** (●), **7** (◆), **8** (▲), **9** (▼), and **10** (■).

was plotted against pH* (Figure 4). Following the so-called "cancel-out approach" for the determination of pK_a values, we did not consider deuterium effects.[27] Application of a correction function developed by Krezel and Bal showed no significant differences.[28] Problems were sometimes encountered because of the precipitation of coordination polymers

(25) (a) Martin, R. B.; Edcall, J. T. *J. Am. Chem. Soc.* **1960**, *82*, 1107. (b) Agarwal, R. P.; Perrin, D. D. *J. Chem. Soc., Dalton Trans.* **1975**, 1045. (c) Sovago, I.; Farkas, E.; Gergely, A. *J. Chem. Soc., Dalton Trans.* **1982**, 2159. (d) Rabenstein, D. L.; Daignault, S. A.; Al Isab, A.; Arnold, A. P.; Shoukry, M. M. *J. Am. Chem. Soc.* **1985**, *107*, 6435. (e) Mlynarz, P.; Kowalik-Jankowska, T.; Stasiak, M.; Leplawy, M. T.; Kozlowski, H. *J. Chem. Soc., Dalton Trans.* **1999**, 3673. (f) Mlynarz, P.; Valensin, D.; Kociolek, K.; Zabrocki, J.; Olejnik, J.; Kozlowski, H. *New J. Chem.* **2002**, *26*, 264.
(26) Ösz, K.; Varnagy, K.; Sovago, I.; Lennert, L.; Süli-Vargha, H.; Sanna, D.; Micera, G. *New J. Chem.* **2001**, 25.
(27) Scheller, K. H.; Scheller-Krattiger, V.; Martin, R. B. *J. Am. Chem. Soc.* **1981**, *103*, 6833.
(28) Krezel, A.; Bal, W. *J. Inorg. Biochem.* **2004**, *98*, 161.

Table 3. Thermodynamic Parameters at 298 K for the Amide Deprotonation Reactions

reaction	pK_a	ΔG, kJ/mol	$\Delta\Delta G$, kJ/mol
6a → **6** (Gly)	8.54 ± 0.02	48.7 ± 0.1	
7a → **7** (Phe)	7.17 ± 0.01	40.9 ± 0.1	−7.8 ± 0.2
8a → **8** (Tyr)	6.85 ± 0.02	39.1 ± 0.1	−9.7 ± 0.2
9a → **9** (Trp)	6.85 ± 0.01	39.1 ± 0.1	−9.7 ± 0.2
10a → **10** (Nal)	6.64 ± 0.09	37.9 ± 0.5	−10.8 ± 0.6

at pH values below 7. It was, therefore, generally better to follow the signals of the N-coordinated species.

Figure 4 clearly indicates that our assumptions concerning π-stacking interactions were correct. The pK_a values that were determined by fitting the curves to a two-state equilibrium are significantly smaller for those complexes having aromatic side chains. π-stacking energies are given by the difference

$$\Delta\Delta G = \Delta G(\mathbf{7}-\mathbf{10}) - \Delta G(\mathbf{6}) \quad (1)$$

They were calculated using the relationship

$$\Delta G = 2.303RT\mathrm{p}K_a \quad (2)$$

The results are summarized in Table 3. They show that aromatic interactions contribute ca. −7 to −11 kJ/mol to the stabilization of the N-coordinated peptide complexes, a range that is comparable to data reported for π−cation interactions.[29] This seems reasonable because a metal-coordinated pyridine ligand is similar to an alkylpyridinium ion. It is interesting that the data on ternary metal amino acid complexes published by Yamauchi et al.[9,10] and Sigel et al.[11] showed a broader range and, in most cases, smaller energies of ca. −2.1 to −10 kJ/mol. The authors have assigned them to normal $\pi-\pi$ stacking. As a result of the larger electrostatic energies involved, π−cation attractions are expected to be significantly stronger than pure $\pi-\pi$ stacking,[1c,30] and $\pi-\pi$ interactions in peptides were experimentally determined to be on the order of ca. −2 to −5 kJ/mol for free enthalpy change.[31] However, several authors have observed π−cation interactions that are as small as ca. −2 to −3 kJ/mol.[32] Furthermore, Fabbrizzi and co-workers have determined stacking energies of −7 to −8 kJ/mol for interactions between anthracene rings and aromatic amino acid side chains in fluorescent zinc complexes.[12] This is comparable to our findings, but unlike the pyridine ligands in **7**−**10**, the anthracene rings are not directly bound to the metal center and, hence, are not cationic. Thus, it is not easy to reach a conclusion concerning the nature of aromatic interactions in metal complexes. We hope that the picture may become clearer with a growing number of data on structurally characterized complexes where important parameters such as the interplane distances between the stacked rings are reasonably well-defined. This study is intended to underline the importance of such data and provide a starting point.

In addition, our findings have implications for the modification of peptides with synthetic metal binding sites. Such compounds are of considerable interest because of their applicability, for example, in biomedicine or catalysis.[33] It may be of particular importance for molecular recognition events in medical applications that noncovalent interactions involving a synthetic ligand can significantly change the secondary structure of a small peptide. Our complexes show that a pyridine ligand suffices to introduce structural motifs that are not known in comparable histidine peptides. Thus, synthetic modifications may help to overcome the lack of secondary structures in small peptides without engineered geometric restrictions and the design of rigid ligands.[34] This could provide a new strategy in the development of enantioselective catalysts that require a sterically well-defined chiral environment.

Conclusions

We have shown that aromatic interactions can result in the unusual folding of small metallopeptides. ^{1}H NMR experiments permitted a quantitative determination of stabilizing free enthalpy changes and confirmed the conformational integrity of the peptides in aqueous solutions. Although it is not yet possible to distinguish between π−cation and $\pi-\pi$-stacking interactions, it is evident that moderate modifications such as the exchange of a histidyl imidazole donor for a pyridine ligand may have considerable consequences for the secondary structure of a synthetic metal complex−peptide conjugate.

Experimental Section

General Methods. Spectra were recorded with the following instruments:

For ^{1}H NMR, a Bruker Advance DPX 300 was used. All chemical shifts are referenced to TSP (trimethylsilylpropionic acid) as an internal standard, with high-frequency shifts recorded as positive. For elemental analysis, a Carlo Erba Elemental Analyzer Model 1106 was used. For FD− and FAB−MS, a Varian MAT 212 was used.

Absolute solvents were purchased from Fluka and stored under nitrogen. Solvents were used without further purification. The water

(29) (a) Kearney, P. C.; Mizoue, L. S.; Kumpf, R. A.; Forman, J. E.; McCurdy, A.; Dougherty, D. A. *J. Am. Chem. Soc.* **1993**, *115*, 9907. (b) Ting, A. Y.; Shin, I.; Lucero, C.; Schultz, P. G. *J. Am. Chem. Soc.* **1998**, *120*, 7135. (c) Hunter, C. A.; Low, C. M. R.; Rotger, C.; Vinter, J. G.; Zonta, C. *Proc. Natl. Acad. Sci. U.S.A.* **2002**, *99*, 4873. (d) Hunter, C. A.; Low, C. M. R.; Vinter, J. G.; Zonta, C. *J. Am. Chem. Soc.* **2003**, *125*, 9936.
(30) Scrutton, N. S.; Raines, A. R. C. *Biochem. J.* **1996**, *319*, 1.
(31) (a) Kiehna, S. E.; Waters, M. L. *Protein Sci.* **2003**, *12*, 2657. (b) Tatko, C. D.; Waters, M. L. *J. Am. Chem. Soc.* **2002**, *124*, 9372. (c) Butterfield, S. M.; Patel, P. R.; Waters, M. L. *J. Am. Chem. Soc.* **2002**, *124*, 9751. (d) Cochran, A. G.; Skelton, N. J.; Starovasnik, M. A. *Proc. Natl. Acad. Sci. U.S.A.* **2001**, *98*, 5578. (e) Cochran, A. G.; Tong, R. T.; Starovasnik, M. A.; Park, E. J.; McDowell, R. S.; Theaker, J. E.; Skelton, N. J. *J. Am. Chem. Soc.* **2001**, *123*, 625. (f) Russell, S. J.; Cochran, A. G. *J. Am. Chem. Soc.* **2000**, *122*, 12600.
(32) (a) Tatko, C. D.; Waters, M. L. *Protein Sci.* **2003**, *12*, 2443. (b) Tsou, L. K.; Tatko, C. D.; Waters, M. L. *J. Am. Chem. Soc.* **2002**, *124*, 14917. (c) Shi, Z. S.; Olson, C. A.; Kallenbach, N. R. *J. Am. Chem. Soc.* **2002**, *124*, 3284. (d) Andrew, C. D.; Bhattacharjee, S.; Kokkoni, N.; Hirst, J. D.; Jones, G. R.; Doig, A. J. *J. Am. Chem. Soc.* **2002**, *124*, 12706. (e) Schneider, H. J.; Blatter, T.; Zimmermann, P. *Angew. Chem., Int. Ed. Engl.* **1990**, *29*, 1161.
(33) (a) Reichert, D. E.; Lewis, J. S.; Anderson, C. J. *Coord. Chem. Rev.* **1999**, *184*, 3. (b) Severin, K.; Bergs, R.; Beck, W. *Angew. Chem., Int. Ed.* **1998**, *37*, 1634. (c) Shimizu, K. D.; Cole, B. M.; Krueger, C. A.; Kuntz, K. W.; Snapper, M. L.; Hoveyda, A. H. *Angew. Chem., Int. Ed. Engl.* **1997**, *36*, 1704. (d) Cole, B. M.; Shimizu, K. D.; Krueger, C. A.; Harrity, J. P. A.; Snapper, M. L.; Hoveyda, A. H. *Angew. Chem., Int. Ed. Engl.* **1996**, *35*, 1668.
(34) Xing, G.; DeRose, V. J. *Curr. Opin. Chem. Biol.* **2001**, *5*, 196.

was bidistilled. All other reagents were of commercially available reagent grade quality. Amino acid derivatives were purchased from Bachem. All other chemicals were from Aldrich. Bis[(2-pyridyl)-methyl]amine (bpa) was prepared according to literature procedures.[35] The syntheses of the ligand Dpg-Phe-OMe[13] and coordination polymers **6a**−**10a**[14,15] were published previously.

Chromatographic separations were achieved on flash columns under nitrogen pressure. The stationary phase was silica (Merck Type 9385, 230−400 mesh, 60 Å) from Aldrich. Technical grade dichloromethane was used after purification by rotary evaporation. Methanol was of p.a. quality. The separation was optimized and followed by thin layer chromatography (silica).

Bromoacetylated Amino Acid Esters. BrAc-Gly-OMe. Gly-OMe·HCl (12.3 g, 98 mmol) was suspended in 200 mL of THF. Triethylamine (27.8 mL, 200 mmol) was added with stirring, and the mixture was cooled to −78 °C in a dry ice bath. Bromoacetylbromide (8.5 mL, 100 mmol) was dissolved in 100 mL of THF, and the solution was added dropwise to the cold suspension over a period of 4 h. The mixture was stirred without further cooling for another 2 h. Upon warming to room temperature, the solution's color turned from yellow to dark brown. Insoluble $HNEt_3Br$ was filtered off through a layer of silica on a glass filter frit, and the solvent was removed to dryness under reduced pressure. The crude dark brown oil was dissolved in ethyl acetate, filtered again through a layer of silica, and washed with an ethyl acetate/*n*-hexane mixture. The brown filtrate was evaporated under a vacuum, and the dry solid residue was purified by silica gel column chromatography using ethyl acetate/*n*-hexane (2:1) as the eluent. A brown fraction containing some amino acid ester starting material eluted first, followed by a broad yellow fraction containing the product. The product fraction was concentrated under a vacuum, and the product was solidified by the addition of diethyl ether to the resulting yellow oil. The white solid material was collected and repeatedly washed with diethyl ether. Recrystallization from ethyl acetate in a refrigerator (−20 °C) overnight afforded the product as colorless block-shaped crystals (1.80 g, 8.6 mmol, 8.60%).

$C_5H_8BrNO_3$ (210.03 g/mol). FAB−MS (nitrobenzyl alcohol) *m*/*z*: 210 [M^+]. ^{1}H NMR (300 MHz, $CDCl_3$): δ 3.79 (s, 3H, OCH_3), 3.92 (s, 2H, Br−CH_2), 4.10 (d, 2H, $^{\alpha}CH_2$), 6.96 (s, br, 1H, NH).

BrAc-Tyr-OMe. L-Tyr-OMe·HCl (5.00 g, 21.6 mmol) was suspended in 100 mL of THF. Triethylamine (6.01 mL, 43.2 mmol) was added with stirring, and the mixture was cooled to −40 °C in a dry ice/methanol/salt bath. Bromoacetylbromide (1.88 mL, 21.6 mmol) was dissolved in 50 mL of THF, and the solution was added dropwise to the cold suspension over a period of 3 h. Stirring was continued for 2 h without further cooling. Insoluble $HNEt_3Br$ was filtered off and the solvent removed under reduced pressure. The crude red-brown oil was purified by silica gel column chromatography using CH_2Cl_2/petrolether (40−60 °C)/MeOH (11:5:1) as the eluent. The product was contained in the second light-yellow fraction. The other layers were not collected. The product fraction was concentrated by rotary evaporation and the resulting yellow oil dried under a vacuum (4.33 g, 13.7 mmol, 63.40%).

$C_{12}H_{14}O_4NBr$ (316.15 g/mol). FD−MS ($CDCl_3$) *m*/*z*: 317 [M^+]. ^{1}H NMR (300 MHz, $CDCl_3$): δ 3.08 (m, 2H, $^{\beta}CH_2$), 3.75 (s, 3H, OCH_3), 3.85 (dd, 2H, Br−CH_2), 4.83 (m, 1H, $^{\alpha}CH$), 5.18 (s, br, 1H, HO−Ph), 6.77 (d, 2H, H2−Ph + H6−Ph), 6.83 (d, br, 1H, NH), 6.97 (d, 2H, H3−Ph + H5−Ph).

BrAc-Trp-OMe. L-Trp-OMe·HCl (4.91 g, 19.3 mmol) was suspended in 150 mL of THF. Triethylamine (5.73 mL, 38.6 mmol) was added with stirring, and the mixture was cooled to −78 °C in a dry ice bath. Bromoacetylbromide (1.68 mL, 19.3 mmol) was dissolved in 100 mL of THF, and the solution was added dropwise to the cold suspension over a period of 2 h. The mixture was stirred for another 2 h without further cooling. The resulting brown mixture was filtered through a glass filter frit with a layer of silica in order to remove insoluble $HNEt_3Br$, and the solvent was removed under reduced pressure until dryness. The crude brown solid was purified by silica gel column chromatography using CH_2Cl_2/MeOH (11:1) as the eluent. A yellow fraction containing some amino acid ester starting material eluted first. The product was contained in the light-yellow second fraction. The other layers were not collected. The solution containing the desired product was concentrated by rotary evaporation. Recrystallization of the residual yellow solid from CH_2Cl_2 overnight in a refrigerator (−20 °C) afforded the product as colorless blocks, which were collected on a sintered-glass filter and dried under a vacuum (4.17 g, 12.3 mmol, 63.73%).

$C_{14}H_{15}BrN_2O_3$ (339.18 g/mol). FAB−MS (nitrobenzyl alcohol) *m*/*z*: 339 [M^+]. ^{1}H NMR (300 MHz, $CDCl_3$): δ 3.37 (m, 2H, $^{\beta}CH_2$), 3.70 (s, 3H, OCH_3), 3.82 (s, 2H, Br−CH_2), 4.91 (m, 1H, $^{\alpha}CH$), 6.94 (d, br, 1H, NH), 7.03 (s, 1H, H6−Ind), 7.14 (m, 2H, H2−Ind + H5−Ind), 7.38 (d, 1H, H4−Ind), 7.55(d, 1H, H7−Ind), 8.16 (s, br, 1H, NH−Ind).

BrAc-2-Nal-OBz: L-2-Nal-OBz·HOTos (HOTos = p-tolylsulfonic acid) (10.12 g, 21.2 mmol) was dissolved in 150 mL of THF followed by addition of triethylamine (5.90 mL, 42.4 mmol) with stirring. The mixture was cooled to −60 °C in a dry ice/acetone/salt bath. Bromoacetylbromide (1.85 mL, 21.2 mmol) was dissolved in 100 mL of THF, and the solution was added dropwise to the cold solution over a period of 4 h. Stirring was continued for 2 h without further cooling. Upon warming to room temperature, the color of the mixture turned form purple to dark blue. Insoluble $HNEt_3Br$ was filtered off through a small layer of silica on a frit and the brown filtrate evaporated to dryness under reduced pressure. The crude brown solid was purified by silica gel column chromatography using CH_2Cl_2/MeOH (11:1) as the eluent. The product was contained in the first yellow fraction. Other fractions were not collected. All solvent was removed by rotary evaporation, and the product was solidified by addition of diethyl ether to the resulting yellow oil. Recrystallization from ethyl acetate in a refrigerator at −20 °C over several days afforded the compound as white pellets, which were collected on a sintered-glass filter and dried under a vacuum (7.89 g, 18.5 mmol, 87.35%).

$C_{22}H_{20}BrNO_3$ (426.30 g/mol). FAB−MS (nitrobenzyl alcohol) *m*/*z*: 426 [M^+]. ^{1}H NMR (300 MHz, $CDCl_3$): δ 3.32 (m, 2H, $^{\beta}CH_2$), 3.83 (s, 2H, Br−CH_2), 4.96 (m, 1H, $^{\alpha}CH$), 5.18 [m, 2H, Bz−CH_2)], 6.91 (d, br, 1H, NH), 7.15 (2d, br, 1H, H3−Nal), 7.25 (m, br, 5H, Bz), 7.47 (m, 3H, H1−Nal + H6−Nal + H7−Nal), 7.70 (m, 2H, H4−Nal + H8−Nal), 7.79 (m, 1H, H5−Nal).

Ligands. General Procedure. Equimolar amounts of bpa, the respective bromoacetylated amino acid ester, and diisopropylethylamine (DIPEA) were dissolved in DMF or CH_3CN. The solution was stirred for 20h at room temperature. All solvents were removed by rotary evaporation. Ethyl acetate was added, resulting in the precipitation of the ammonium halide salt, which was filtered off and discarded. The filtrate was concentrated to dryness, yielding brown oil, which was purified on a silica gel column using CH_2Cl_2/MeOH (11:1) as the eluent. A small yellow fraction containing some amino acid starting material eluted first. The product followed in a broad light-yellow fraction. Other layers were not collected. The product fraction was concentrated to dryness by rotary evaporation and the resulting brown oil dried under a vacuum.

Dpg-Gly-OMe. 1.00 g (4.8 mmol) of BrAc-Gly-OMe, 0.95 g (4.8 mmol) of bpa, 9 mL of DIPEA, 30 mL of CH_3CN, 30 mL of AcOEt. Yield: 1.17 g (3.6 mmol, 74.77%). $C_{24}H_{26}N_4O_4$ (328.39

(35) (a) Hojland, F.; Toftlund, H.; Yde-Andersen, S. *Acta Chem. Scand.* **1983**, *A37*, 251. (b) Romary, J. K.; Zachariasen, R. D.; Barger, J. D.; Schiesser, H. *J. Chem. Soc., Dalton Trans. (C)* **1968**, 2884.

g/mol). FD−MS ($CDCl_3$) *m/z*: 329 [M^+]. ^{1}H NMR (300 MHz, $CDCl_3$): δ 3.31 [s, 2H, C(O)CH_2], 3.65 (s, 3H, OCH_3), 3.82 (s, 4H, 2 × py−CH_2), 4.04 (d, 2H, $^{\alpha}CH_2$), 7.10 (m, 2H, H4−py), 7.28 (d, br, 2H, H3−py), 7.55 (m, 2H, H5−py), 8.49 (d, 2H, $^3J_{H,H}$ = 4.90 Hz, H6−py).

Dpg-Tyr-OMe. 2.56 g (8.1 mmol) of BrAc-Tyr-OMe, 1.61 g (8.1 mmol) of bpa, 1.41 mL (8.1 mmol) of DIPEA, 50 mL of DMF, 50 mL of AcOEt. Yield: 2.62 g, (6.0 mmol, 74.45%). $C_{24}H_{26}N_4O_4$ (434.49 g/mol). FD−MS ($CHCl_3$) *m/z*: 435 [M^+]. ^{1}H NMR (300 MHz, $CDCl_3$): δ 2.98−3.21 (m, 2H, $^{\beta}CH_2$), 3.70 [s, 2H, C(O)-CH_2], 3.74, 3.82 (2d, 4H, 2 × py−CH_2), 4.89 (m, 1H, $^{\alpha}CH$), 6.34 (d, 2H, H2−Ph + H6−Ph), 6.94 (d, 2H, H3−Ph + H5−Ph), 7.24 (m, 4H, H3−py + H5−py), 7.59 (m, 2H, H4−py), 8.51 (d, 2H, H6−py), 9.09 (d, 1H, NH).

Dpg-Trp-OMe. 3.37 g (9.9 mmol) of BrAc-Trp-OMe, 1.97 g (9.9 mmol) of bpa, 1.73 mL (9.9 mmol) of DIPEA, 50 mL of DMF, 50 mL of AcOEt. Yield: 3.01 g (6.6 mmol, 66.41%). $C_{26}H_{27}N_5O_3$ (457.52 g/mol). FD−MS ($CDCl_3$) *m/z*: 458 [M^+]. ^{1}H NMR (300 MHz, CD_3CN): δ 3.20 [dd, 2H, C(O)CH_2], 3.37 (m, 2H, $^{\beta}CH_2$), 3.65 (s, 3H, OCH_3), 3.72, 3.79 (2d, 4H, $^2J_{H,H}$ = 13.94 Hz, 2 × py−CH_2), 4.79 (m, 1H, $^{\alpha}CH$), 7.06−7.19 (m, 7H, 2 × H3−py + H4−py + 2 × H5−py + H5−Ind + H6−Ind), 7.43 (d, 1H, H2−Ind), 7.61 (m, 3H, H4−Ind + H7−Ind + H4−py), 8.50−8.52 (2d, 2H, $^3J_{H,H}$ = 4.53 Hz, 2 × H6−py), 8.81 (d, br, 1H, NH−amide), 9.36 (s, br, NH−Ind).

Dpg-2-Nal-OBz. 2.01 g (4.7 mmol) of BrAc-2-Nal-OBz, 0.94 g (4.7 mmol) of bpa, 0.82 mL (4.7 mmol) of DIPEA, 100 mL of CH_3CN, 100 mL of AcOEt. Yield: 2.05 g (3.8 mmol, 79.74%). $C_{34}H_{32}N_4O_3$ (544.64 g/mol). FD−MS ($CDCl_3$) *m/z*: 544 [M^+]. ^{1}H NMR (300 MHz, $CDCl_3$): δ 3.23 [s, 2H, C(O)CH_2], 3.31−3.48 (m, 2H, $^{\beta}CH_2$), 3.67, 3.75 (2 d, 4H, 2 × py−CH_2), 5.05 (m, 1H, $^{\alpha}CH$), 5.09−5.19 (m, 2H, Bz−CH_2), 7.01−7.05 (m, 4H, H3−Nal + H7−Nal + 2 × H3−py), 7.19−7.29 (m, 8H, Bz + H5−py + H6−Nal), 7.41 (m, 2H, H4−py), 7.57−7.66 (m, 3H, H1,4,8-Nal), 7.74 (d, br, 1H, H5−Nal), 8.44 (d, 2H, H6−py), 9.13 (d, 1H, NH).

[(Dpg-Xaa-OMe)(H_2O)Zn](CF_3SO_3)$_2$ (1, 3−5). General Procedure. Solid $Zn(CF_3SO_3)_2$ was added to a stirred solution of 1 equiv of the respective ligand in CH_3CN. Stirring at room temperature continued overnight followed by the removal of all of the solvent under a vacuum. CH_2Cl_2 was added to the residue and the resulting suspension left in refrigerator (−20 °C) overnight. Unchanged $Zn(CF_3SO_3)_2$ precipitated and was filtered off. The product obtained after stripping all of the solvent from the filtrate was dried under a vacuum and used without further purification.

[(Dpg-Gly-OMe)(H_2O)Zn](CF_3SO_3)$_2$ (1). 1.29 g (3.9 mmol) of bpaAc-Gly-OMe, 1.43 g (3.9 mmol) of $Zn(CF_3SO_3)_2$, 50 mL of CH_3CN, 50 mL of CH_2Cl_2. Yield: 2.4 g (3.5 mmol, 88.26%). $C_{19}H_{22}F_6N_4O_{10}S_2Zn$ (709.91 g/mol). FAB−MS (nitrobenzyl alcohol) *m/z*: 541 [(M − CF_3SO_3)$^+$]. ^{1}H NMR (300 MHz, CD_3CN): δ 3.60 (s, 3H, OCH_3), 3.82 [s, 2H, C(O)CH_2], 3.95 (d, 2H, $^2J_{H,H}$ = 5.85 Hz, $^{\alpha}CH_2$), 4.32 (s, 4H, py−CH_2), 7.58 (d, 2H, H5−py), 7.65 (m, 2H, H3−py), 8.09 (m, 2H, H4−py), 8.24 (s, br, 1H, NH), 8.70 (d, 2H, H6−py). C, H, N, S Elem Anal. Calcd for **1**: C, 32.98; H, 2.91; N, 8.10; S, 9.27%. Found: C, 32.73; H, 2.69; N, 7.99; S, 9.20%.

[(Dpg-Tyr-OMe)(H_2O)Zn](CF_3SO_3)$_2$ (3). 1.87 g (4.3 mmol) of bpaAc-Tyr-OMe, 1.56 g (4.3 mmol) of $Zn(CF_3SO_3)_2$, 100 mL of CH_3CN, 50 mL of CH_2Cl_2. Yield: 2.80 g (3.4 mmol, 79.80%). $C_{26}H_{28}F_6N_4O_{11}S_2Zn$ (816.03 g/mol). FAB−MS (nitrobenzyl alcohol) *m/z*: 649 [(M − CF_3SO_3 − H_2O)$^+$]. ^{1}H NMR (300 MHz, CD_3-OD): δ 2.58−2.95 (m, 2H, $^{\beta}CH_2$), 3.58−3.75 [m, 5H, OCH_3 + C(O)CH_2], 4.39−4.54 (5H, 2 × py−CH_2 + $^{\alpha}CH$), 6.51 (m, 2H, H2−Ph + H6−Ph), 6.67 (m, H3−Ph + H5−Ph), 7.66 (m, 4H, H3−py + H5−py), 8.12 (m, 2H, H4−py), 8.53−8.60 (2d, 2H, $^3J_{H,H}$ = 5.31 Hz, H6−py). C, H, N, S Elem Anal. Calcd for **3**: C, 38.27; H, 3.46; N, 6.87; S, 7.63%. Found: C, 39.26; H, 3.59; N, 6.67; S, 7.63%.

[(Dpg-Trp-OMe)(H_2O)Zn](CF_3SO_3)$_2$ (4). 2.05 g (4.5 mmol) of bpaAc-Trp-OMe, 1.63 g (4.5 mmol) of $Zn(CF_3SO_3)_2$, 100 mL of CH_3CN, 100 mL of CH_2Cl_2. Yield: 3.33 g (88.34%). $C_{28}H_{29}F_6N_5O_{10}$-S_2Zn (839.07 g/mol). FAB−MS (nitrobenzyl alcohol) *m/z*: 670 [(M − CF_3SO_3 − H_2O)$^+$]. ^{1}H NMR (300 MHz, CD_3CN): δ 2.92 (H_2O), 3.00−3.08 (2d, 1H, $^{\beta}CH_2$), 3.25−3.30 (2d, 1H, $^{\beta}CH_2$), 3.49−3.55 (d, 1H, py−CH_2), 3.56 [s, 2H, C(O)CH_2], 3.64 (s, 3H, OCH_3), 4.01−4.19 (3d, 3H, py−CH_2), 4.88 (m, 1H, $^{\alpha}CH$), 6.96 (m, 4H, H2,3,4,6-Ind), 7.40 (m, 1H, H5−Ind), 7.50 (m, 2H, H5−py), 7.62 (m, 2H, H3−py), 8.11 (m, 2H, H4−py), 8.18 (d, br, 1H, NH), 8.51−8.61 (2d, 2H, H6−py), 9.17 (s, br, 1H, NH−Ind). C, H, N, S Elem Anal. Calcd for **4**·2H_2O: C, 38.39; H, 3.77; N, 7.99; S, 7.31%. Found: C, 37.68; H, 3.06; N, 8.56; S, 7.32%.

[(Dpg-2-Nal-OBz)(H_2O)Zn](CF_3SO_3)$_2$ (5). 2.00 g (3.7 mmol) of bpaAc-2-Nal-OBzl, 1.33 g (3.7 mmol) of $Zn(CF_3SO_3)_2$, 100 mL of CH_3CN, 100 mL of CH_2Cl_2. Yield: 3.00 g (3.2 mmol, 88.26%). $C_{36}H_{34}F_6N_4O_{10}S_2Zn$ (926.19 g/mol). FAB−MS (nitrobenzyl alcohol) *m/z*: 757 [(M − CF_3SO_3 − H_2O)$^+$]. ^{1}H NMR (300 MHz, $CDCl_3$): δ 2.91−3.00 (m, 1H, $^{\beta}CH_2$), 3.29−3.37 [m, 5H, $^{\beta}CH_2$ + C(O)CH_2 + H_2O], 3.55 (d, 1H, py−CH_2), 3.75−3.96 (m, 2H, py−CH_2), 4.24 (d, 1H, py−CH_2), 4.96−5.07 [m, 3H, $^{\alpha}CH$ + Bz−CH_2], 6.80−7.84 (m, br, 18H, H3,4,5-py + Nal + Bz), 8.49−8.70 (2d, 2H, H6−py), 9.05 (d, 1H, NH). C, H, N, S Elem Anal. Calcd for **5**: C, 46.68; H, 3.70; N, 6.05; S, 6.92%. Found: C, 46.82; H, 3.36; N, 6.27; S, 7.63%.

Synthesis of [(Dpg-Xaa)$^{-H}$Zn] (6−10). General Procedure. The tetrameric complex {[(Dpg-Gly)Zn](CF_3SO_3)}$_4$ (**6a**)[16] and the polymers {[(Dpg-Xaa)Zn]$_3$(CF_3SO_3)$_3$}$_\infty$ (Xaa = Phe, **7a**; Tyr, **8a**; Trp, **9a**; Nal, **10a**) were synthesized as described previously[14,15] for **7a**, **8a,** and **10a** and were used as starting materials. The respective complex was dissolved in H_2O and the pH adjusted to 9.00 with 1 M NaOH. The mixture was stirred overnight and the solvent removed by rotary evaporation. The residual solid material was dried under a vacuum and purified by reprecipitation from methanol or ethanol. Bulk samples obtained by this method contained variable quantities of $NaCF_3SO_3$ or water, as is evident from elemental analysis and mass spectrometry data. The reported yields are based on the C, H, N, S elemental analysis data of a characteristic sample. Crystals for X-ray structure analyses of [(Dpg-Phe)Zn]$_\infty$ (**7**), [(Dpg-Tyr)Zn]$_\infty$ (**8**), and {[(Dpg-2-Nal)Zn]·Na(CF_3-SO_3)}$_\infty$ (**10**) were grown by slow diffusion of diethyl ether into methanol solutions. Single crystals of [(Dpg-Trp)Zn] (**9**) were obtained after several weeks at room temperature from an aqueous NaOH solution at pH 8.00.

[(Dpg-Gly)$^{-H}$Zn] (6). 400 mg (0.24 mmol) of {[(Dpg-Gly)Zn]-(CF_3SO_3)}$_4$, 15 mL of H_2O. Yield: 220 mg (0.40 mmol, 41.7%). $C_{16}H_{16}N_4O_3Zn$ (*M* = 377.71 g/mol). FAB−MS (nitrobenzyl alcohol) *m/z*: 399 [(M + Na)$^+$], 377 [M^+]. ^{1}H NMR (300 MHz, D_2O/NaOD; pH* = 9.00): δ 3.44 [s, br, 2H, C(O)CH_2], 3.82 (s, br, 2H, $^{\alpha}CH_2$), 4.28 (s, br, 4H, py−CH_2), 7.16 (m, 4H, H3,5-py), 8.09 (m, 2H, H4−py), 8.65 (d, 2H, H6−py). ^{1}H NMR (300 MHz, D_2O/DCl; pH* = 4.00): δ 3.74 [s, br, 2H, C(O)CH_2], 3.82 (s, br, 2H, $^{\alpha}CH_2$), 4.42 (m, 4H, py−CH_2), 7.58 (m, 4H, H3,5-py), 8.06 (m, 2H, H4−py), 8.66 (d, 2H, H6−py). C, H, N, S Elem Anal. Calcd for **6**·$NaCF_3SO_3$·0.5H_2O: C, 36.51; H, 3.04; N, 10.02; S, 5.72%. Found: C, 36.66; H, 3.70; N, 9.99; S, 4.89%.

[(Dpg−Phe)$^{-H}$Zn] (7). 500 mg (0.26 mmol) of {[(Dpg-Phe)-Zn]$_3$(CF_3SO_3)$_3$}$_\infty$, 30 mL of H_2O. Yield: 304 mg (0.58 mmol, 74.3%). $C_{23}H_{22}N_4O_3Zn$ (M = 467.84 g/mol). FAB−MS (nitrobenzyl alcohol) *m/z*: 489 [(M + Na)$^+$], 467 [M^+]. ^{1}H NMR (300 MHz, D_2O/NaOD; pH* = 9.00): δ 3.17 [m, 3H, $^{\beta}CH_2$, C(O)CH_2], 3.57

[d, 1H, C(O)CH_2], 3.77, 3.83 (2d, 2H, py−CH_2), 4.35 (m, 3H, $^{\alpha}$CH, py−CH_2), 6.44 (m, 1H, H4−Ph), 6.75 (m, 2H, H3,5-Ph), 6.90 (m, 2H, H2,6-Ph), 7.49 (m, 4H, H3,5-py), 8.02 (m, 3H, H4,6-py), 8.42 (d, 1H, H6−py). ^{1}H NMR (300 MHz, D_2O/DCl; pH* = 4.00): δ 2.69 (dd, 1H, $^{\beta}CH_2$), 3.11 (dd, 1H, $^{\beta}CH_2$), 3.61 [m, 2H, C(O)CH_2], 3.97 (d, 1H, py−CH_2), 4.35 (m, 4H, $^{\alpha}$CH, py−CH_2), 7.03 (m, 4H, H2,3,5,6-Ph), 7.57 (m, 4H, H3,5-py), 8.06 (m, 2H, H4−py), 8.56 (d, 2H, H6−py), 8.61 (d, 2H, H6−py). C, H, N Elem Anal. Calcd for **7**·3H_2O: C, 52.93; H, 5.41; N, 10.74%. Found: C, 53.16; H, 5.01; N, 10.81%.

[**(Dpg-Tyr)$^{-H}$Zn**] **(8).** 300 mg (0.15 mmol) of {[(Dpg-Tyr)Zn]$_3$-(CF_3SO_3)$_3$}$_\infty$, 15 mL of H_2O. Yield: 190 mg (0.38 mmol, 81.79%). $C_{23}H_{22}N_4O_4Zn$ (M = 483.84 g/mol). FAB−MS (nitrobenzyl alcohol) m/z: 505 [(M + Na)$^+$], 483 [M$^+$]. ^{1}H NMR (300 MHz, D_2O/NaOD; pH* = 9.00): δ 2.93 [m, 3H, $^{\beta}CH_2$ + C(O)CH_2], 3.38 [d, 1H, C(O)CH_2], 3.69 (d, 2H, py−CH_2), 4.14 (m, 3H, $^{\alpha}$CH, py−CH_2), 6.06 (d, 2H, H2,6-Ph), 6.59 (d, 2H, H3,5-Ph), 7.36 (m, 4H, H3,5-py), 7.87 (m, 3H, H4,6-py), 8.27 (d, 1H, H6−py). ^{1}H NMR (300 MHz, D_2O/DCl; pH* = 4.00): δ 2.58 (dd, 1H, $^{\beta}CH_2$), 3.07 (dd, 1H, $^{\beta}CH_2$), 3.60 [m, 2H, (N)CH_2(CO)], 3.88 (d, 1H, py−CH_2), 4.33 (m, 4H, $^{\alpha}$CH, py−CH_2), 6.52 (m, 2H, H2,6-Ph), 6.89 (m, 2H, H3,5-Ph), 7.54 (m, 4H, H3,5-py), 8.04 (m, 2H, H4−py), 8.56 (d, 1H, H6−py), 8.63 (d, 1H, H6−py). C, H, N Elem Anal. Calcd for **8**·0.5H_2O: C, 56.00; H, 4.66; N, 11.36%. Found: C, 56.07; H, 3.84; N, 11.27%.

[**(Dpg-Trp)$^{-H}$Zn**] **(9).** 230 mg (0.11 mmol) of {[(Dpg-Trp)Zn]$_3$-(CF_3SO_3)$_3$}$_\infty$, 10 mL of H_2O. Yield: 150 mg. $C_{25}H_{23}N_5O_3Zn$ (M = 506.87 g/mol). FAB−MS (nitrobenzyl alcohol) m/z: 506 [M$^+$]. ^{1}H NMR (300 MHz, D_2O/NaOD; pH* = 9.00): δ 3.08 [d, 1H, C(O)CH_2], 3.29 (d, 1H, py−CH_2), 3.36 (d, 1H, $^{\beta}CH_2$), 3.48 (d, 1H, py−CH_2), 3.51 (m, 1H, $^{\beta}CH_2$), 3.69 (d, 1H, py−CH_2), 3.89 [d, 1H, C(O)CH_2], 4.16 (m, 1H, py−CH_2), 4.37 (m, 1H, $^{\alpha}$CH), 6.82 (d, 1H, H6−Ind), 6.95 (m, 3H, H2,4,5-Ind), 7.17 (d, 1H, H5−py), 7.39 (m, 4H, H3,5,6-py), 7.92 (m, 3H, H4−py + H7−Ind), 8.41 (d, 1H, H6−py). ^{1}H NMR (300 MHz, D_2O/DCl; pH* = 4.00): δ 2.91 (m, 1H, $^{\beta}CH_2$), 3.40 [m, 4H, $^{\beta}CH_2$, C(O)−CH_2, py−CH_2], 4.03 (d, 2H, py−CH_2), 4.22 (d, 1H, py−CH_2), 4.69 (m, 1H, $^{\alpha}$CH), 7.05 (m, 4H, H4,5,6,7-Ind), 7.46 (m, 5H, H3,5-py, H1−Ind), 7.99 (m, 2H, H4−py), 8.39 (d, 1H, H6−py), 8.59 (d, 1H, H6−py).

Alternative Synthesis. Analytically pure samples of **9** were obtained by the following method: Equimolar amounts of Dpg-Trp-OMe (1.06 g, 2.32 mmol) and sodium hydroxide (0.10 g, 2.32 mmol) were dissolved in 50 mL of CH_3OH. The solution was stirred for 2h at room temperature, and the solvent was removed by rotary evaporation. The dry residue was dissolved in 50 mL of water, and the pH was adjusted to pH 9.00 with 2 M NaOH. After stirring overnight, 1 M HCl was added to adjust the pH to 5.00. All water was removed by rotary evaporation. Methanol was added to the dry residue, resulting in the precipitation of NaCl salt, which was filtered off through a 0.2 μ filter. The filtrate was concentrated to dryness, yielding a light-yellow solid, which was purified by recrystallization from methanol/diethyl ether. Yield: 0.64 g (1.38 mmol, 59.77%). C, H, N Elem Anal. Calcd for Dpg-Trp-OH·H_2O, $C_{25}H_{27}N_5O_4$ (461.51 g/mol): C, 65.06; H, 5.90; N, 15.17. Found: C, 65.35; H, 5.70; N, 14.63.

Solid $ZnCl_2$ (153 mg, 1.13 mmol) was added to a stirred solution of Dpg-Trp-OH (499 mg, 1.13 mmol) in 50 mL of H_2O. The pH was adjusted with 2 M NaOH to 9.00. Precipitating excess zinc salts were filtered off, and the clear solution was stirred overnight. The pH was set to 8.00 using 1 M HCl, and water was removed by rotary evaporation. The crude product was dried in a vacuum and redissolved in methanol. Insoluble NaCl was filtered off, and diethyl ether was added to the clear filtrate until the product started to precipitate. The resulting suspension was left overnight in a deep freezer at −20 °C. The product [(Dpg-Trp-O)Zn]·2CH_3OH (487 mg, 0.96 mmol, 85.0%) was collected on a sintered-glass filter funnel and dried under a vacuum. The methanol content was confirmed by ^{1}H NMR spectroscopy. Other spectroscopic data are in agreement with those of the material obtained as described above. C, H, N Elem Anal. Calcd for $C_{27}H_{31}N_5O_5Zn$: C, 56.80; H, 5.47; N, 12.27%. Found: C, 56.89; H, 5.66; N, 12.68%.

[**(Dpg-2-Nal)$^{-H}$Zn**] **(10).** 400 mg (0.19 mmol) of {[(Dpg-2-Nal)-Zn]$_3$(CF_3SO_3)$_3$}$_n$, 15 mL of H_2O. Yield: 230 mg (0.22 mmol, 38.6%). $C_{27}H_{24}N_4O_3Zn$·CF_3NaO_3S (M = 667.02 g/mol). FAB−MS (nitrobenzyl alcohol) m/z: 539 [(M − CF_3SO_3)$^+$], 517 [**10**$^+$]. ^{1}H NMR (300 MHz, D_2O/NaOD; pH* = 9.00): δ 3.07 [d, 1H, C(O)CH_2], 3.33 (m, 2H, $^{\beta}CH_2$), 3.55 [m, 2H, py−CH_2, C(O)CH], 4.09 (2H, py−CH_2), 4.39 (m, 1H, $^{\alpha}$CH), 6.58 (d, 2H, H6,7-Nal), 7.03 (d, 1H, H3−Nal), 7.25 (m, 6H, H4,5,8-Nal, H3,5-py), 7.44 (m, 4H, H1−Nal, H3,4,6-py), 7.90 (m, 1H, H4−py), 8.32 (d, 1H, H6−py). ^{1}H NMR (300 MHz, D_2O/DCl; pH* = 4.00): δ 2.79 (dd, 1H, $^{\beta}CH_2$), 3.38 (dd, 1H, $^{\beta}CH_2$), 3.55 [m, 4H, C(O)−CH_2, py−CH_2], 4.34 (m, 3H, $^{\alpha}$CH, py−CH_2), 7.06−7.75 (m, 11H, H−naphthyl, H3,5-py), 7.96 (m, 1H, H4−py), 8.05 (m, 2H, H4−py), 8.23 (d, 1H, H6−py), 8.54 (d, 1H, H6−py). C, H, N, S Elem Anal. Calcd for **10**·3$NaCF_3SO_3$: C, 34.84; H, 2.34; N, 5.42; S, 9.30%. Found: C, 34.69; H, 2.64; N, 5.41; S, 8.83%.

^{1}H NMR Titrations. The respective complex was dissolved in 14 mL of D_2O, and the pH was adjusted with NaOD in D_2O to ca. 9 in the cases of **7**−**10** and ca. 10 in the case of **6**. A total of 200 μL of a 20% DCl/D_2O solution were diluted with 5 mL of D_2O. This solution was used to lower the pH in steps of ca. 0.2−0.5. At each step, an NMR sample was collected and set aside for measurement.

X-ray Crystallography. A summary of the crystallographic data and structure refinement details is given for all compounds in Table 1 (also see the Supporting Information). Intensity data (Mo Kα, λ = 0.710 73 Å) were collected on a Bruker-Nonius Kappa CCD diffractometer. Semiempirical absorption corrections based on equivalent reflections were made using the program SADABS.[36] All structures were solved by direct methods and refined using full matrix least-squares procedures on F^2 using the program package SHELXTL NT 6.12.[37,38] Non-hydrogen atoms were anisotropically refined. H atoms were fixed in geometrically calculated positions (riding mode) with an isotropic displacement parameter of 1.2 or 1.5 times that of the respective C, O, or N atom. One of the methanol molecules in {**7**·2.5CH_3OH}$_\infty$ is disordered on a crystallographic 2-fold rotation axis. It was refined without H atoms. Details have been deposited at the Cambridge Crystallographic Data Centre as supplementary publications CCDC numbers 255842 ({**7**·2.5CH_3OH}$_\infty$), 255843 ({**8**}$_\infty$), 255844 (**9**), and 255845 (**10**·Na-(CF_3SO_3)$_\infty$). Copies are available free of charge from CCDC, 12 Union Road, Cambridge CB2 1 EZ (UK) [Fax: (+44)1223−336033; E-mail: deposit@ccdc.cam.ac.uk].

Acknowledgment. We thank Dr. Nicole Niklas for the synthesis of bis[(2-pyridyl)methyl]amine. Financial support by the Deutsche Forschungsgemeinschaft (SFB 583) is gratefully acknowledged.

Supporting Information Available: Crystallographic data available in CIF format. This material is available free of charge via the Internet at http://pubs.acs.org.

IC0500053

(36) *SADABS*; Bruker-AXS, Inc.: Madison, WI, 2002.
(37) *SHELXTL NT*, version 6.12; Bruker-AXS, Inc.: Madison, WI, 2002.
(38) Flack, H. D. *Acta Crystallogr., Sect. A* **1983**, *A39*, 876.